

July 2009, for *The Astrophysical Journal*

## X-ray and Radio Variability of M31\*, The Andromeda Galaxy Nuclear Supermassive Black Hole

Michael R. Garcia<sup>1</sup>, Richard Hextall<sup>1,2</sup>, Frederick K. Baganoff<sup>3</sup>, Jose Galache<sup>1</sup>, Fulvio Melia<sup>4</sup>, Stephen S. Murray<sup>1</sup>, Frank A. Primini<sup>1</sup>, Loránt O. Sjouwerman<sup>5</sup>, and Ben Williams<sup>6</sup>

### ABSTRACT

We confirm our earlier tentative detection of M31\* in X-rays and measure its light-curve and spectrum. Observations in 2004-2005 find M31\* rather quiescent in the X-ray and radio. However, X-ray observations in 2006-2007 and radio observations in 2002 show M31\* to be highly variable at times. A separate variable X-ray source is found near P1, the brighter of the two optical nuclei. The apparent angular Bondi radius of M31\* is the largest of any black hole, and large enough to be well resolved with Chandra. The diffuse emission within this Bondi radius is found to have an X-ray temperature  $\sim 0.3$  keV and density  $0.1 \text{ cm}^{-3}$ , indistinguishable from the hot gas in the surrounding regions of the bulge given the statistics allowed by the current observations. The X-ray source at the location of M31\* is consistent with a point source and a power law spectrum with energy slope  $0.9 \pm 0.2$ . Our identification of this X-ray source with M31\* is based solely on positional coincidence.

*Subject headings:* accretion — black hole physics — galaxies: individual (M31)  
— galaxies: nuclei

---

<sup>1</sup>Harvard-Smithsonian Center for Astrophysics, 60 Garden Street, Cambridge, MA 02138; garcia@head.cfa.harvard.edu

<sup>2</sup>Department of Physics, University of Southampton, UK

<sup>3</sup>Kavli Institute for Astrophysics and Space Research, Massachusetts Institute of Technology, Cambridge MA 02138

<sup>4</sup>Physics Department, The Applied Math Program, and Steward Observatory, The University of Arizona, Tucson AZ 85721

<sup>5</sup>National Radio Astronomy Observatory, Socorro NM 87801

<sup>6</sup>Department of Astronomy, University of Washington, Seattle WA 98195

## 1. Introduction

SMBHs in galactic nuclei spend the vast majority of their life accreting at very low rates, but our understanding of how this accretion occurs is relatively poor compared to our understanding of what happens at high rates. At high rates a slim accretion disk often forms and  $\sim 10\%$  of the accretion energy is radiated. At low rates the accretion becomes radiatively inefficient, but we are uncertain what fraction of the accretion energy is radiated, and what fraction of the gas accreted at large radii actually reaches the black hole event horizon.

While it is clear that some sort of a radiatively inefficient accretion flow (RIAF) occurs, its form as a magnetically dominated inflow Shvartsman (1971); Melia (1992a), an ADAF (Advection Dominated Accretion Flow; Narayan & Yi (1994)), CDAF (Convective Dominated Accretion Flow in which advection occurs but is moderated by convection; Igumenshchev et al. (2000); Narayan et al. (2000); Quataert & Gruzinov (2000)), an ADAF & wind (in which a large fraction of the accreted material is blow out in a wind before reaching the SMBH; Narayan & Yi (1995)); sometimes called an ADIOS (Advective Dominated Inflow Outflow Solution; Blandford & Begelman (1999); Hawley & Balbus (2002)), or something else is unclear. One of the most promising ways to determine which of these alternatives is correct is to image the accretion flow on a sub-Bondi scale and therefore determine the structure of the flow. Spectra taken on sub-Bondi scale would also be highly discriminating.

Perhaps the best candidate for such a study is the SMBH in M31, called hereafter M31\*. The mass of M31\* has previously been estimated as  $3 \times 10^7 M_{\odot}$  (Kormendy & Bender 1999), but more recent HST spectroscopy indicates the mass is  $1.4^{+0.7}_{-0.3} \times 10^8 M_{\odot}$  (Bender et al. 2005). This higher mass means the Bondi radius is not the  $0.9''$  previously estimated (Garcia et al. 2005) but  $\sim 5''$  (see below), making it the largest of any known SMBH (see Figure 1). Within the Bondi radius Chandra detects several point sources and also diffuse gas which is present throughout the bulge of M31 (Shirey et al. 2001a; Takahashi et al. 2004; Li & Wang 2007a). Our earlier work (Garcia et al. 2000) suggested that a super-soft point source near the nucleus was the X-ray counterpart of M31\*, but subsequent alignment with M31 globular clusters (Barmby & Huchra 2001) revealed that this was not the case (Garcia et al. 2001, 2005). *Chandra* HRC imaging revealed that the X-ray source closest to the nucleus is made up of two partially resolved components, one of which is within  $\sim 0.1''$  of the position of P3 and which we tentatively identified as the  $\sim 10^{36}$  erg s $^{-1}$  X-ray counterpart of M31\* (Garcia et al. 2005). In this work we confirm the detection and measure the variability of this SMBH.

Hubble imaging revealed an unusual double nucleus within M31 (Lauer et al. 1993) which has been successfully modeled as an eccentric torus of stars viewed nearly edge on

(Tremaine 1995). The optically brighter end of the torus is known as P1, the optically fainter (but UV brighter) end as P2. More recent Hubble imaging and spectroscopy revealed that embedded within P2 is a dense cluster of several hundred A-stars which are very UV bright. This cluster has been dubbed P3 and its brightness peaks at essentially the same position as that of P2 (Bender et al. 2005). HST spectroscopy reveals a dark mass (presumed black hole) located at the center of this cluster with an estimated mass of  $1.4_{-0.3}^{+0.7} \times 10^8 M_{\odot}$  (Bender et al. 2005). The presence of so many young A stars in the nucleus of M31, which otherwise is made up of an old stellar population, is a mystery. The same phenomenon is also seen near Sgr A\* (Ghez et al. 2003a). Demarque & Virani (2007) suggest that these apparently young stars may actually be old and relics of stellar collisions in the very dense nuclear regions, but recent HST spectra indicate that at least in the case of the Galactic center these are genuine young, massive stars (Ghez et al. 2003b; Martins et al. 2008). A suggested source for the gas which later collapses to form the P3 star cluster is stellar mass loss from the older stars in the orbiting torus (Chang et al. 2007).

Spitzer imaging reveals that M31 looks less like a spiral galaxy than previously thought. Instead, the warm gas and dust is in the form of a set of rings, apparently due to transits of M32 through the center of the plane of the M31 disk (Barmby et al. 2006; Gordon et al. 2006). The most recent of these transits took place 210 million years ago (Block et al. 2006), and would have triggered a burst of star formation.

The association of the radio source ( $\sim 30 \mu\text{Jy}$  at 3.6 cm) with a nuclear black hole by Crane et al. (1993) and Melia (1992b) and subsequently by all others so far is supported by the detection of an unresolved ( $< 1$  pc or  $0.35''$ ) radio source at the position of the stellar nucleus (within  $\sim 1/2''$ , Garcia et al. (2005)), and radio variability which is comparable to the radio variability of Sgr A\* (Sjouwerman et al. 2005).

While M31\* is 100x further away than the SMBH in the center of our Galaxy, it suffers much less reddening:  $A_V \sim 1$  (Garcia et al. 2000), whereas  $A_V \sim 30$  for Sgr A\*. The dominant temperature of the diffuse gas in the core of M31 is  $\sim 0.3$  keV (Dosaj et al. (2001); Shirey et al. (2001b); Li & Wang (2007b); Bogdan & Gilfanov (2008)) as compared to 1.0 keV (Baganoff et al. 2003) around Sgr A\*. A comparative study of these two closest SMBH (M31\* and Sgr A\*) will deepen our understanding of the physics of black hole accretion and emission mechanisms at low rates. In this regard, M31\* and Sgr A\* offer interesting differences in that M31\* is 3x less luminous in the radio but 1 to 3 orders of magnitude more luminous in the X-ray.

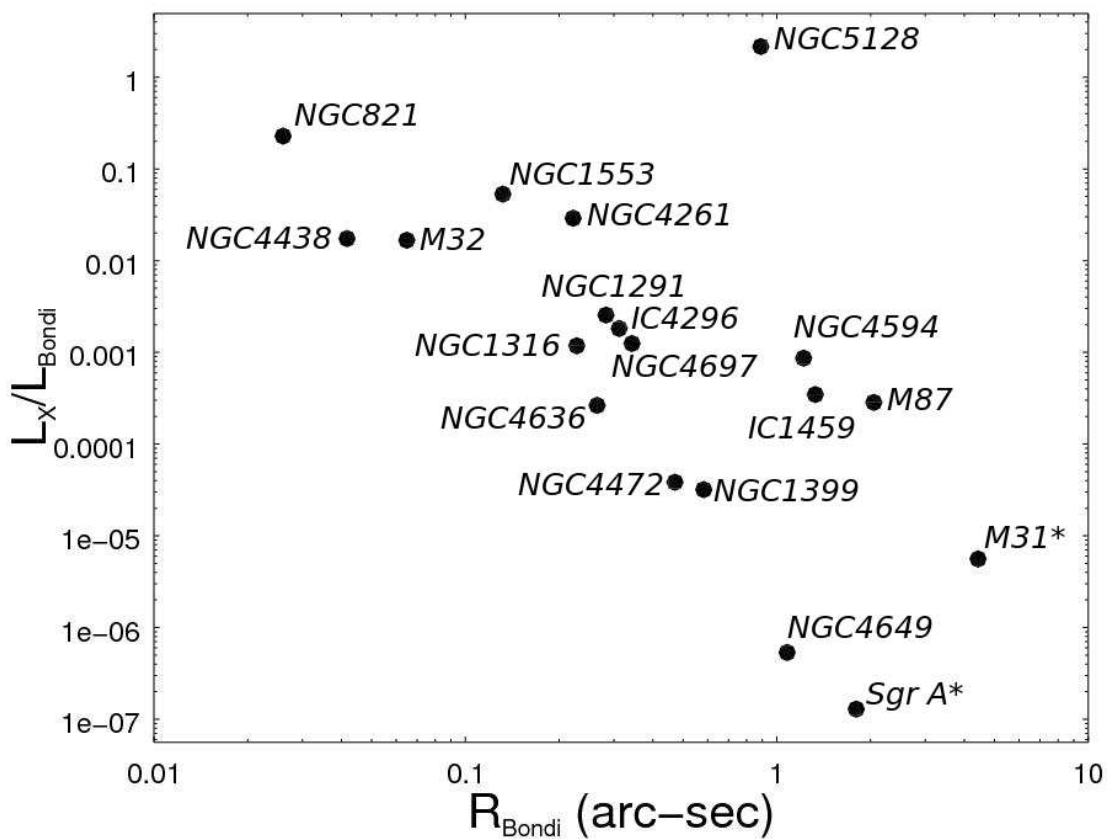


Fig. 1.— The Bondi radii of nearby SMBH vs. their apparent X-ray luminosity (or upper limits) in units of the expected Bondi luminosity. Objects in the lower right of this diagram provide simultaneously secure and severe constraints on accretion and emission models for these SMBH. In this regard, M31\* is the outstanding object.

## 2. Observations

M31 has been observed extensively with both *Chandra* (i.e., Garcia et al. (2000); Kong et al. (2003); Williams et al. (2006); Di Stefano et al. (2004)) and XMM-Newton (i.e., Shirey et al. (2001b); Pietsch et al. (2007)). Many of the *Chandra* observations have been in the form of monthly short ( $\sim 5$  ks) snap-shots in order to monitor the variability of the point source population, but there also have been longer observations to search for rapid variability (Kaaret 2002) and to study source populations (Di Stefano et al. 2004; Pietsch et al. 2007). The total *Chandra* exposure on M31 is now  $\sim 1.3$ Ms and it continues to climb. If one limits the selection of data to only those taken with ACIS-I within 1 arcmin of the nucleus, the total exposure is currently  $\sim 250$  ks. While *Chandra* is able to view M31 10 months out of every year, visibility from XMM-Newton is restricted to a few week long window every 6 months, so the XMM-Newton observations have taken the form of less frequent, but longer, exposures (Trudolyubov et al. 2005).

The *Chandra* observations discovered the first resolved SNR in an external galaxy (Kong et al. 2002a), and summed *Chandra* observations have provided a fiducial point for X-ray color-color diagrams which help to separate unresolved X-ray source populations in more distant galaxies into SNR, high and low mass X-ray binaries, and background AGN (Kong et al. 2002b; Prestwich et al. 2003). These data-sets have also revealed extensive structure in the diffuse emission (Li & Wang 2007b; Bogdan & Gilfanov 2008). Multi-wavelength studies of the M31\* environment suggests the presence of an outflow of hot gas from the nuclear region Li et al. (2009).

Below we discuss the data-sets analyzed in this paper; first those taken with the *Chandra* HRC and then those taken with the *Chandra* ACIS.

### 2.1. Chandra HRC Observations

In 2004/2005 we undertook a series of 4 moderate (50ks) HRC-I exposures separated by 1 month in order to confirm our earlier possible detection of M31\* and to search for any variability. Two of these exposures were subdivided into approximately equal sections and separated by the normal 10 hour pause in observations while *Chandra* transits the Earth's radiation belts. We also include in our analysis archival HRC observations made during 2006/2007 which were designed to monitor optical nova (Henze et al. 2009), and a single 50 ks observation from 2001 (Kaaret 2002). Table 1 lists the data-set we have analyzed, giving observation dates and exposure times.

In order to identify M31\* within the *Chandra* images and then extract a light-curve, it

Obs-id	Start Date (mm/dd/yy)	Exposure Time (ks)
1912	11/01/01	50.0
5925	12/06/04	46.7
6177	12/27/04	20.2
5926	12/27/04	28.5
6202	01/28/05	18.2
5927	01/28/05	27.2
5928	02/21/05	45.2
7283	06/05/06	20.1
7284	09/30/06	20.2
7285	11/13/06	18.7
7286	03/11/07	19.1
8526	11/07/07	20.2
8527	11/17/07	20.2
8528	11/28/07	20.2
8529	12/07/07	19.1
8530	12/17/07	20.1

Table 1: This table shows the Observation ID’s, Dates and Exposure Times for the 16 *Chandra* HRC images discussed in this paper.

was first necessary to accurately determine the location of M31\* within the HRC images. The absolute astrometric accuracy of HST and *Chandra* images is  $\lesssim 1''$ , which is insufficient to uniquely identify sources in the crowded core of M31. Within narrow fields ( $\lesssim 1'$ ) it is possible to register HST and *Chandra* images to  $\sim 0.1''$  accuracy (Edmonds et al. 2003). Over larger fields the PSF of the *Chandra* mirror increases substantially, and this along with the calibration of the HRC may limit the astrometric accuracy even with registration (Beckerman et al. 2004).

There are very few sources in common between our *Chandra* images and the HST/ACS (F435W) images which show the M31 double nucleus, so we used a 2 step process to register our images. As part of our search for counterparts to black hole X-ray transients (Williams et al. 2005) we obtained several HST/ACS images of the M31 nucleus, and one of these was first registered to the Local Group Survey (Massey et al. 2006) image of M31. The second step is to register the *Chandra* images to the same LGS image. We allow for an x and y translation, a single change in scale factor, and roll, but typically the latter two of these are negligible while the translation is significant and  $< 1''$ .

The HST/ACS to LGS registration typically uses 20 stars and has a RMS of  $0.03''$ , and the registration of individual Chandra/HRC images to the LGS uses 6 or 7 globular clusters and has a rms of  $0.1'' - 0.2''$ . One of these 7 globular clusters sometimes falls below the *Chandra* detection threshold, limiting us to 6 occasionally. We note that there are 9 globular clusters which are in both the *Chandra* and LGS images, but 2 of these are between  $6'$  and  $10'$  from the nucleus where the PSF due to the *Chandra* mirror has widened substantially. Including these distant clusters increases the error in the registration to  $\sim 0.3''$ , so we have excluded them. The remaining clusters are between  $1'$  and  $5'$  from the nucleus. Clearly the *Chandra* to LGS registration error dominates the final registration, and this error itself is dominated by the counting statistics within the PSF (and associated registration errors) in the individual globular clusters within the *Chandra* images.

In order to ensure the most accurate, and perhaps more importantly, stable, registration, we summed the HRC data into a single image and registered that image to the LGS images. The summing process (CIAO *reproject\_aspect*) uses the positions of bright X-ray sources to register the individual HRC images to a common frame to better than  $0.05''$ . The accuracy of the registration of the summed Chandra image to the LGS image as determined with IRAF *ccmap* is  $0.1''$  rms. We also summed the 2001/2004/2005 and 2006/2007 HRC data separately and registered these two images to the LGS, again finding a rms accuracy of  $0.1''$ . Comparing these two (now registered) HRC images to each other, we find an offset between bright sources of  $0.2''$ , larger than the formal error in the rms. Given that we are solving for 4 parameters (x and y shift, scale factor, and roll) with 7 points, the resulting formal rms might not be expected to be Gaussian - we therefore take  $0.2''$  as our de-facto registration error between the HST and *Chandra* images.

These two images are shown in Figure 2. The 2006/2007 image shows two separate X-ray sources at the approximate locations of P1 and P3. A simple translation of  $0.25''$  brings the Southwestern source to the position of P3, and the Northeastern source  $0.1''$  to the South of P1. Given the concurrence between the separation of the X-ray sources, the angle between them, and P1 and P3 as seen in the HST images, we identify the X-ray sources with M31\* (=P3) and a source within P1. This concurrence can also be seen in Figure 3, which shows the HST/ACS image with the HRC contours overlaid. However, we cannot entirely exclude the possibility that one or more transient sources unrelated to P1 or P3 are responsible for the X-ray emission.

Since counting statistics of the globular clusters in the individual  $\sim 20$  ks X-ray images limit the accuracy of the registration, we rely on the registration of the merged 430 ks image and measure offsets to P1 and P3 from the nearby super-soft source (CXO J004244.2+411608, Garcia et al. (2000); hereafter SSS). The SSS has between 100 and 300 counts in each of the

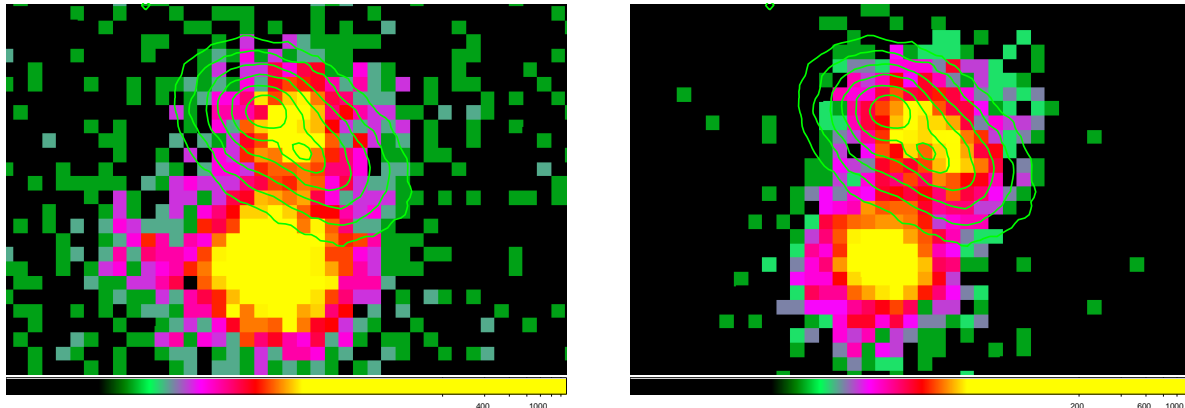


Fig. 2.— The summed 2001/2004/2005 (left) and 2006/2007 (right) HRC images of the M31 nucleus, registered to a common astrometric frame. The registration is accurate to  $\sim 0.2''$ . The contours are from an HST/ACS image. The innermost contour levels are closed at the positions of P1 (upper left, or North-East) and P3 (lower right) and are separated by  $0.5''$ . In the 2004/2005 image the source associated with P3 (=M31\*) is faint, while in the 2006/2007 image this source is stronger and clearly separate from the source near P1. The super-soft source CXO J004244.2+411608 (Garcia et al. 2000) is the bright source directly South of P1/P3.

images, so can be centroided to  $\sim PSF/\sqrt{(counts)} \sim 0.05''$  in each of the individual images.

In order to extract the HRC light-curves we centered extraction circles at the locations of P1 and P3 as determined by the offsets from the SSS (after the translation of  $0.25''$  discussed above) on each of the images and counted the photons therein. We used radii of  $0.4''$  centered at P1 and P3, as shown in Figure 4. P1 and P3 are sufficiently close that these circles overlap, so we excluded the counts in the overlapping region.

Figure 5 shows the resulting light-curves. There is clearly some correlation between the P1 and P3 light-curves, as is expected due to the proximity of the two sources. The  $0.4''$  extraction circle contains 50% of the flux from a point source and the two sources are only  $0.5''$  apart.

The most dramatic variability we find is in December 2007 (day 519 to 529), where M31\* varies by a factor of 3 in 10 days. The maximum variability is between day 117 and 519, where we see a factor of more than 10 variation. In order to search for variability on short timescales, we divided the day 519 observation (where M31\* was brightest) into 5 approximately equal 4000 s intervals. Figure 6 shows the resulting light-curve. While there are apparent  $\sim 2\sigma$  deviations, a  $\chi^2$  test to the hypothesis of a constant source has a 6% chance of being satisfied, so significant variability cannot be convincingly argued.

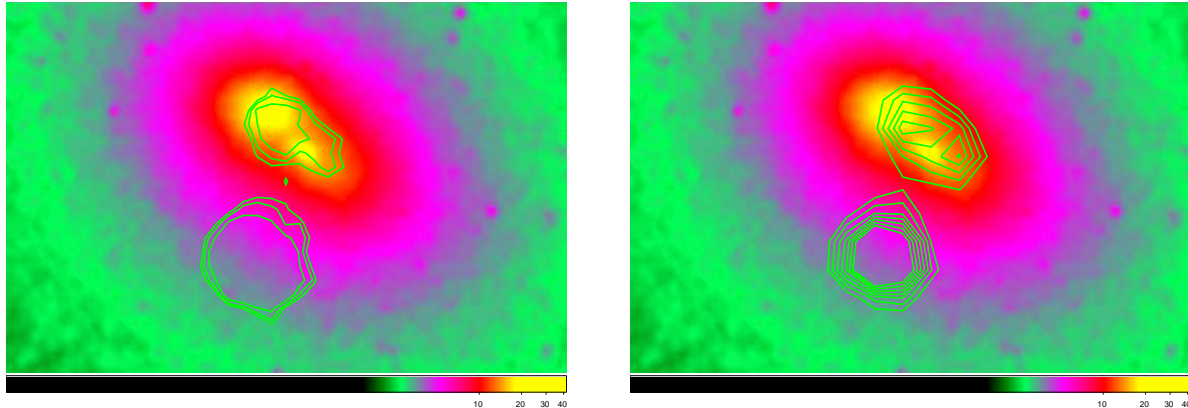


Fig. 3.— A false color representation of the HST/ACS F435W image of the M31 nucleus, with the contours from the HRC images overlaid. The left image shows the contours from the summed 430ks HRC data. The right image shows the contours from the 2006/2007 HRC data alone. A small East-West translation will bring the X-ray peaks on top of P3 and within  $0.1''$  of P1.

In order to test the sensitivity of the light-curve to possible errors in the registration, we shifted the extraction circles  $0.05''$  both RA and DEC, as this is the typical error in measuring the centroid of the SSS which is used as the reference point. While the overall character of the resulting light-curve remains the same, some of the points do see  $> 2\sigma$  changes (see Figures 5 and 6).

Assuming the spectral shape found with ACIS (see below) of  $\alpha_\nu = 0.9$  and  $N_{\text{H}} = 6 \times 10^{20} \text{ cm}^{-2}$ , a measured rate of 1.0 c/ks corresponds to an emitted luminosity over 0.3 – 7.0 keV of  $2.25 \times 10^{36} \text{ erg s}^{-1}$  in the full HRC beam, or  $3.0 \times 10^{36} \text{ erg s}^{-1}$  over 0.1 – 7.0 keV. M31\* therefore ranges in luminosity from 0.6 –  $20 \times 10^{36} \text{ erg s}^{-1}$  (0.1 – 7.0 keV). We note that if the source we associate with M31\* is in fact unrelated, then these number are upper limits and the X-ray luminosity of M31\* must at times be below  $6 \times 10^{35} \text{ erg s}^{-1}$ .

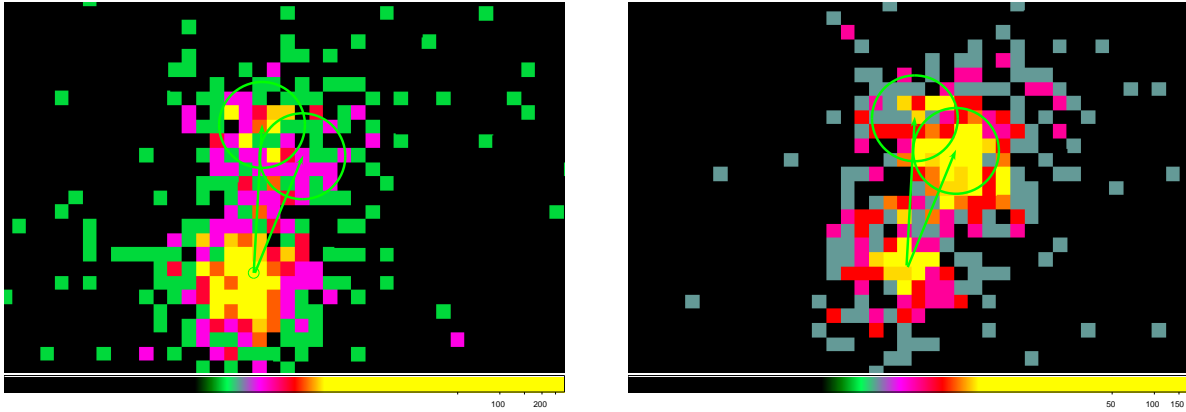


Fig. 4.— Two of the 15 HRC images used in our light-curves. The left image from 2004 Dec 6.75 shows the source at P1 somewhat brighter than that at P3, while the right image from 2008 Dec 7 shows P3 at its brightest. The  $0.4''$  circles used to measure the counts are re-centered for each observation by using an identical set of vectors positioned to originate at the centroid of the super-soft source CXO J004244.2+411608 (Garcia et al. 2000) seen at the bottom of the images. Light curves were generated from the counts in these  $0.4''$  circles, excluding counts from the overlapping region.

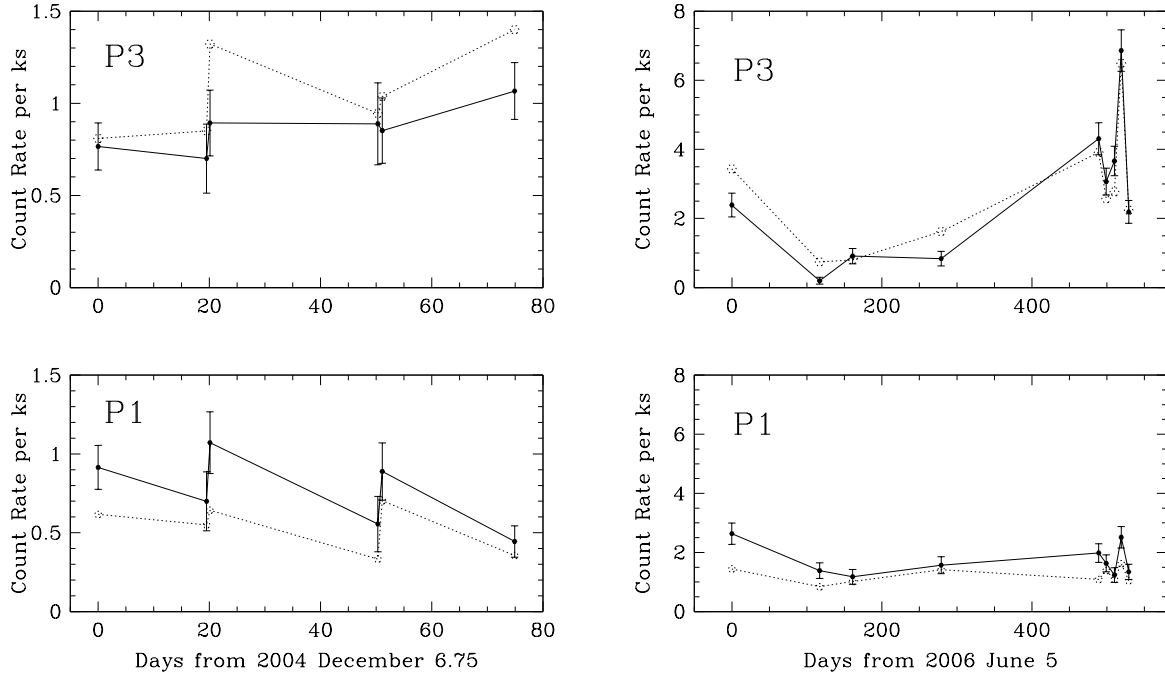


Fig. 5.— Light-curves for P3 = M31\* and the source near P1 as extracted from our 2004/2005 HRC data (left) and archival 2006/2007 (right) HRC data. A counting rate of 1.0 counts per ks corresponds to a luminosity of  $3 \times 10^{36}$  erg  $s^{-1}$  (0.1 – 7.0 keV) at the 780 kpc distance of M31. Error-bars are  $1\sigma$  counting statistics only. The dashed line indicates the sensitivity of the light-curve to  $1\sigma$  shifts in the registration and therefore count extraction procedure. We do not include the 2001 observation in the light-curve due to its 3 year offset.

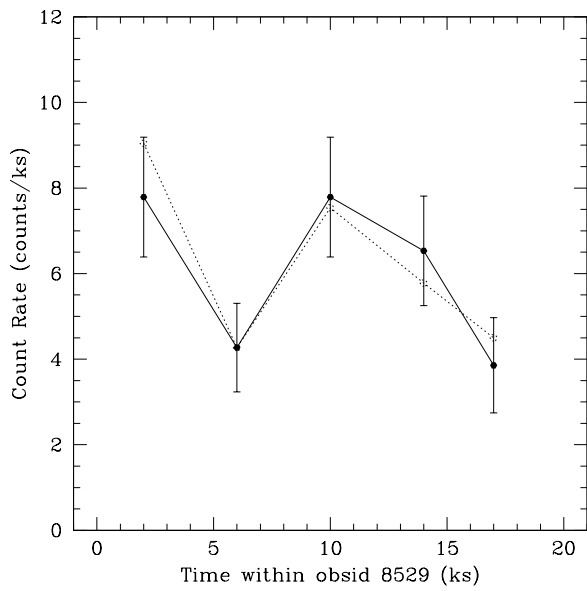


Fig. 6.— Light-curve for P3 = M31\* during obsid 8529 (day 529 in Figure 5). The data were divided into 4000 sec intervals in order to measure the rate. While there are  $\sim 2\sigma$  deviations, a  $\chi^2$  test to a constant source finds  $\chi^2/\nu = 8.87/4$ , which has a 6% chance of originating from a constant source. Short time scale variability is therefore not detected. As before, the dashed line and points represent the light-curve extracted from slightly shifted positions.

## 2.2. Chandra ACIS

While the HRC data gives excellent spatial resolution and allows us to determine an accurate light-curve for M31\*, They do not provide sufficient energy resolution to allow us to search for spectral signatures of the Bondi flow/ADAF. We therefore investigate the archival ACIS-I and ACIS-S data.

We used 29 ACIS-I exposures aimed within 1' of M31\* which total to 148ks of exposure time. This summed exposure is shown in Figure 7 (left) as a smoothed 3-color X-ray image where the soft (0.3-1.0 keV), medium (1.0-2.5 keV), and hard (2.5-7.0 keV) bands are color coded as red, green, and blue respectively. The 5'' Bondi radius is shown here in green. The emission due to hot diffuse gas is seen throughout this image and generates  $\sim 1$  event per pixel in this image. Note that we do not include the ACIS-S observation discussed below, obsid 1575, in this sum due to the substantially different energy response of ACIS-S vs. ACIS-I.

We searched for an enhancement in the flux at (or inside) of the Bondi radius by generating radial profiles of the flux, centered on M31\* , in several wedges that are free of point sources. Defining the ray to the North as zero degrees and moving counterclockwise, we generated these profiles over the azimuth ranges of 40 to 70 degrees, 100 to 150 degrees, and 245 to 280 degrees. In the first two of these azimuth ranges we found a slight excess of counts near the Bondi radius (above the local background), amounting to 10 counts from 3'' to 5'' in the first region and 20 counts from 4'' to 6'' in the second region. We then used MARX to estimate the number of counts that would be scattered into these regions from the surrounding point sources, and found that this could account for  $\sim 1/3$  of the observed excess. Note that there is clear spatial structure in the diffuse emission at larger radii (10'' – 20'', see Li et al. (2009)) which, if present at or within the Bondi radius, could easily account for the apparent excess of 10 to 20 counts seen in two of our regions. Assuming that the results in these three azimuth ranges are typical of what would be found for the diffuse emission at all azimuth ranges, and given that these three ranges sum to  $\sim 1/3$  of the total, we take the apparent excess of 30 total counts to correspond to a limit three times higher, or  $\sim 100$  counts, on any truly diffuse emission due to the Bondi flow. This limit corresponds to an emitted flux of less than  $9 \times 10^{-15}$  erg cm $^{-2}$  s $^{-1}$ (0.3-7.0 keV) assuming a temperature of 0.3 keV, or a luminosity at 780 kpc of  $< 6 \times 10^{35}$  erg s $^{-1}$ .

Given that we do not detect a significant enhancement in the flux at (or inside) the Bondi radius, we would not expect to detect a temperature change either as any such change would need to be co-incidentally offset by a change in electron density. None the less, we did select energy bands of Figure 7 such that approximately equal counts are produced in the soft and medium bands in order that any change in the  $\sim 0.3$  keV temperature of the

Obs-id	Start Date (mm/dd/yy)	Exposure Time (ks)
303	10/13/99	11.8
305	12/11/99	4.1
306	12/27/99	4.1
307	01/29/00	4.1
308	02/16/00	4
311	07/29/00	4.9
312	08/27/00	4.7
1581	12/13/00	4.4
1582	02/18/01	4.3
1583	06/10/01	4.9
4360	08/11/02	4.9
4678	11/09/03	3.9
4679	11/26/03	3.8
4680	12/27/03	4.2
4681	01/31/04	4.2
4682	05/23/04	3.9
4719	07/17/04	4.1
4720	09/02/04	4.1
4721	10/04/04	4.1
4722	10/31/04	3.8
7064	12/04/06	23.2
7136	01/06/06	4
7137	05/26/06	3.9
7138	06/09/06	4.1
7139	07/31/06	4
7140	09/24/06	4.1
8183	01/14/07	4
8184	02/14/07	4.1
8185	03/10/07	4

Table 2: This table shows the Observation ID's, Dates, Start Times and Exposure Times for the 29 ACIS-I images merged together and shown in Figure 7 (left). Total exposure time is 148 ks.

diffuse gas would be emphasized. As evidenced by the lack of a color change in Figure 7, there is no apparent change in the temperature of the diffuse gas at the Bondi radius.

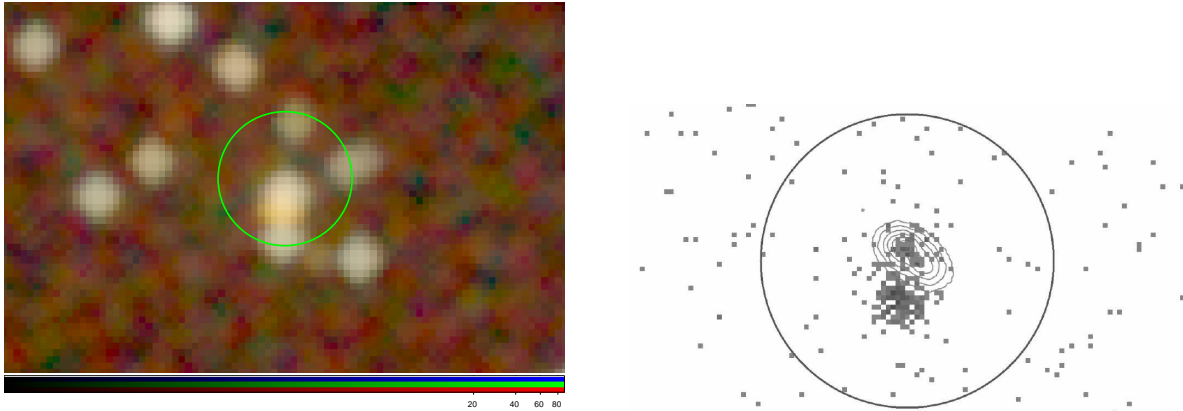


Fig. 7.— (left) The smoothed, summed, 148 ks exposure ACIS-I image centered on M31\*. The circle is the 5'' Bondi radius. The color coding shows the soft band in red (0.3–1.0 keV), the medium band in green (1.0–2.5 keV) and the hard band in blue (2.5–7.0 keV). There is no clear change in the temperature of the diffuse gas at or inside of the Bondi radius. The low temperature of the super-soft source immediately to the South of M31\* is apparent by its yellowish color. (right): The longest single ACIS-S exposure of M31\* is this 40ks exposure (obsid 1575). The HST/ACS F435W contours are overlaid and the 5'' Bondi radius is shown. Pixel size has been set to 0.125'' to match the HRC images shown earlier.

Because spectral fitting summed ACIS data spanning many years consisting of 29 separate observations is not straightforward, we carried out a spectral analysis with the longest single ACIS observation of M31\*, OBSID 1575. This 40 ks ACIS-S exposure is shown in Figure 7 (right), with Bondi radius and also the HST contours overlaid. Extracting the counts in a 0.4'' radius centered at M31\* and excluding the overlapping region centered at P1 we find 70 counts and find a good fit to a power-law spectrum of the form  $F_{\nu,x} \propto \nu^{-\alpha_{\nu,x}}$  with energy index  $\alpha_{\nu,x} = 0.9 \pm 0.4$  and  $N_H$  consistent with Galactic value of  $6 \times 10^{20} \text{ cm}^{-2}$ . Freezing  $N_H$  to be equal to the Galactic value we are able to place a tighter constraint on  $\alpha_{\nu,x} = 0.9 \pm 0.2$ .

Extracting the diffuse counts within the Bondi radius, and excluding the point sources, we find 182 counts. Fits to a single component model do not yield acceptable  $\chi^2$ , but fits to a power-law (which is suitable to represent the undetected point sources and the small amount of scattering from the detected point sources) and a thermal spectrum are acceptable. Freezing the power-law to  $\alpha_{\nu,x} = 0.7$  and  $N_H$  to  $6 \times 10^{20} \text{ cm}^{-2}$  (consistent with the Galactic value) yields a good fit ( $\chi^2 = 1.3$  with 9 dof) with  $kT = 0.34 \pm 0.05$ . The density within this region, assuming a 5'' radius sphere, is measured to be  $\sim 0.1 \text{ cm}^{-3}$ .

### 2.3. VLA

We observed M31\* simultaneously with the VLA at 5 GHz during our 2004/2005 Chandra/HRC observations. Figure 8 (right) shows the day-long averages of the radio flux observed during these observations. We did not see any significant variability within the day long averages, to a limit of 15% on timescales of 2, 4, and 6 hours. On other occasions M31\* has shown variability on several hour long timescales, as can be seen in Figure 8 (left). Here the hypothesis of a constant source can be rejected at the 99.99% confidence level ( $\chi^2/\nu = 43.1/11$ ). This high confidence level is due almost entirely to the two measurements of zero flux in 2002 July 06, as if we disregard those measurements the hypothesis of a constant source is acceptable at the 24% confidence level ( $\chi^2/\nu = 11.6/9$ ).

M31\* has been observed at several radio wavelengths from the VLA, but not at the same time. Because the source is variable determining a spectrum from these observations is uncertain, but it is all the current data will allow. The mean flux densities observed at the VLA are  $\sim 30 \mu\text{Jy}$  at 8.4 GHz (measured on 1990 July, 1992 November, 1994 July, 1995 July, 1996 January),  $\sim 50 \mu\text{Jy}$  at 4.9 GHz (measured on 2002 July & August, 2003 June, July & August, and during our monitoring simultaneous with Chandra in 2004 December, 2005 January & February) and between 100 and 140  $\mu\text{Jy}$  at 1.4 GHz (measured on 1981 August, 1986 August & September). The beam size varies from 0.24'' to 0.4'' to 1.4'', respectively at these frequencies, so one must also beware that if there is any diffuse emission it would elevate the fluxes at the lower frequencies, however the available images do not show any such emission. Taken at face value these flux densities indicate a slope  $\alpha_{\nu,r} = 0.8$ , where  $F_{\nu,r} \propto \nu^{-\alpha_{\nu,r}}$ .

## 3. Discussion

### 3.1. A Random Superposition?

While we have detected X-ray emission at a location consistent with M31\* which we argue does indeed originate from M31\*, we must also ask what the chances are of a random X-ray binary within the nuclear region of M31 being located at the position of P3=M31\*? In order to answer this question one needs to estimate the density of sources in the nuclear region. As the density increases with decreasing radius one needs to assume some fiducial radius within which to compute the density.

We take the Bondi radius as this fiducial radius. We then count the number of sources within this radius both in M31, and also in our Galaxy under the assumption that the density

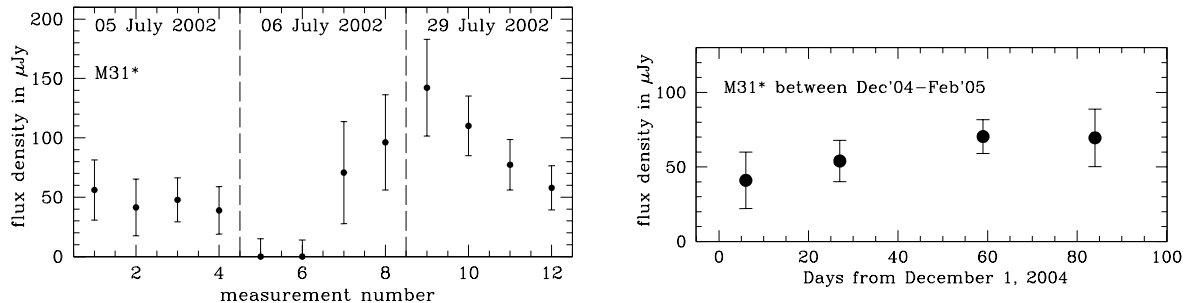


Fig. 8.— (left) The 2-hour averaged radio variability of the nuclear source M31\* in three 8-hour 6 cm VLA B-configuration observations during 2002 (Sjouwerman et al. 2005). During the first half of the second observation M31\* was not detected, while it was detected during the second half, implying significant variability on a few hour long time scale. (right) The day-long VLA averages at 5 GHz from our simultaneous radio/X-ray observations during 2004/2005. Variability on the few hour long time scale seen in 2002 is not evident in any of these 4 individual observations, suggesting that M31\* may have been in a different (non-variable?) state during 2004/2005.

of bright nuclear sources is similar. Within the Galaxy, the number of  $> 10^{36}$  erg  $\text{s}^{-1}$  at the M31\* Bondi radius if it was transferred to the Galaxy (ie, within  $100 \times 5''$ ) is two (Wijnands et al 2008). Given this number, the probability of a random source being within  $0.2''$  (the registration/centroiding error) of M31\* is 0.3%. If we count sources  $> 10^{36}$  erg  $\text{s}^{-1}$  within the Bondi radius at M31 itself, we find 4 (or 5, depending upon the epoch) and a probability of 0.6%. We note that these numbers are conservative, because if we increase the fiducial radius by 3.2x and therefore the surface area by 10x, the average source density and therefore probability decreases by 5x.

While the odds of an interloper are small, we note that there is nothing in the X-ray spectrum of light curve of the source at P3 to distinguish it from an interloping X-ray binary. Our identification of this source as M31\* is based solely on positional coincidence. The variations in luminosity that we have found of  $0.6 - 20 \times 10^{36}$  erg  $\text{s}^{-1}$  (0.1-7.0 keV) are consistent with the upper limit of  $1.2 \times 10^{36}$  erg  $\text{s}^{-1}$  set by Li et al. (2009), particularly considering that M31\* was relatively faint in the 2004/2005 observations.

As well as confirming our tentative detection of M31\* (Garcia et al. 2005), we have detected variable emission consistent with a location in P1. The emission could be due to a single low mass X-ray binary embedded in P1.

### 3.2. Bondi Rate

We have previously estimated the Bondi accretion rate (Garcia et al. 2005). Herein we update that estimation using the same methods. We measure the temperature of the diffuse gas within  $5''$  of M31\* to be  $0.34 \pm 0.05$  keV, consistent with what has been previously measured in the inner  $\sim 1'$  (Takahashi et al. 2004; Li & Wang 2007a; Bogdan & Gilfanov 2008). This temperature and the new mass estimate lead to a Bondi radius of  $5.2''$  at 780 kpc. The density in the inner  $1''$  has been estimated at  $0.06 \text{ cm}^{-3}$  (Li & Wang 2007a) and  $0.1 \text{ cm}^{-3}$  (Takahashi et al. 2004; Dosaj et al. 2001). Herein we find a density of  $0.1 \text{ cm}^{-3}$  within the Bondi radius, leading to a Bondi accretion rate of  $7 \times 10^{-5} M_{\odot}\text{yr}^{-1}$  and a Bondi luminosity of  $4 \times 10^{41} \text{ erg s}^{-1}$ . Given the observed luminosity of  $\sim 2 \times 10^{36} \text{ erg s}^{-1}$  this leads to an under luminosity of  $5 \times 10^{-6}$  as shown in Figure 1.

While the Bondi rate is the standard with which to compare SMBHs and to search for evidence of RIAFs, it assumes that the gas is stationary at the Bondi radius. Winds from stars, supernovas, or other sources may modify the Bondi rate if they are at high enough velocity (Melia 1992a). Bogdan & Gilfanov (2008) suggest that SNR drive a bipolar wind out of the plane of M31 with a speed of  $\sim 60 \text{ km s}^{-1}$ . This wind is seen at large distances from M31\*, but if it extends to, or originates in, the nuclear region of M31 it still should not greatly effect the Bondi flow because its velocity is a factor of five lower than the sound speed of  $\sim 300 \text{ km s}^{-1}$ . On the other hand, if the bipolar flow centers on M31\* then there may be some connection with outflows or jets originating from the RIAF.

### 3.3. Variability

In the X-ray, the most rapid variability which is clearly detected is a factor of 3 on a 10 day timescale. This is consistent with the orbital timescale at  $\sim 100$  Schwarzschild radii ( $r_S = 2GM/c^2$ ) from M31\*. X-ray flares are seen in Sgr A\* with durations of hours and amplitudes of a factor of  $\sim 10$  (Baganoff et al. 2001; Marrone et al. 2008). Given that we would expect the time scale of such flares to scale with mass, similar flares in M31\* would occur on a  $\sim 40$  hour or a few day long time scales. Thus this most rapid variability we see from M31\* might plausibly be associated with the flares seen in Sgr A\*.

Figure 6 shows an (unsuccessful) attempt to detect X-ray variability on even shorter time scales. If we had detected variability on very short time scales it might be taken as evidence that the X-ray emission was not from M31\*, but from an interloping X-ray binary. However, we caution here that the  $2r_S$  light crossing time for M31\* is  $\sim 1/3$  hour, so one would have to detect variations on time scales shorter than this in order to argue against an

origin in M31\*.

In the radio, we detect more rapid variability than in the X-ray. In particular, during the first half of an 8 hour observation on 2002 July 06 M31\* is undetected and during the second half it is clearly detected. This implies variability of at least a factor of 2 on several hour time scales. Sgr A\* typically shows only 10% to 40% variability in the radio on time scales as short as a day Brown & Lo (1982); Macquart & Bower (2006). Given this, the variations we see on 06 July 2002 are unusual.

The spectral slope of the emission from M31\* appears to be the same in the radio and X-ray frequency ranges, but the X-ray flux is far above the extension of the radio spectrum into the X-ray range. As is the case with Sgr A\*, this energy distribution is consistent with a synchrotron source for the radio emission and Compton up-scattering of the radio photons by the relativistic electrons into the X-ray range in synchrotron self Compton or SSC process (Falcke & Markoff 2000; Liu & Melia 2001; Hornstein et al. 2007). If this is indeed the emission mechanism, then the short timescale radio variability should be echoed in the X-ray flux. Despite the fact that we did not detect X-ray variability on this short timescale during the observations presented herein, the X-ray counting rate when M31\* is at its brightest is sufficient to suggest that future observations may detect this.

### 3.4. Accretion Flow

Sgr A\* appears to be a slightly resolved (non point) source in the Chandra images with a luminosity of  $\sim 10^{34}$  erg  $s^{-1}$ . This implies that the accretion flow itself is bright in X-rays. In contrast, in M31\* there is no discernible difference in the X-ray emission within the Bondi radius. It appears consistent with that from the diffuse gas in the larger surrounding area. Unfortunately, it is unclear whether we would even detect the accretion flow around Sgr A\* if it was at the distance of M31\*. The fractional Eddington luminosity of an ADAF flow scales with fractional Eddington mass accretion rate (see for example Figure 7 of Narayan & McClintock (2008)). M31\* and Sgr A\* are accreting at approximately the same Eddington scaled rate, so the Sgr A\* flow would be  $\sim 50$ x brighter around M31\* due to its higher mass, or  $\sim 5 \times 10^{35}$  erg  $s^{-1}$ . This is on the order of the upper limit to excess diffuse emission due to the Bondi flow that we derived above. However, it is important to note that any prediction based on a Sgr A\*-like ADAF is uncertain by at least an order of magnitude because the 0.1 – 1.0 keV X-ray luminosity of the Sgr A\* flow is hidden behind  $10^{23}$   $cm^{-2}$  of absorption.

If we accept that the A-stars in P3 are from a recent star formation episode then age

of the P3 star cluster may be  $\sim 200$  Myr (Bender et al. 2005), and the mass required to produce this cluster during a single star formation burst may be between a few  $10^4 M_\odot$  and  $10^6 M_\odot$  (Bender et al. 2005; Chang et al. 2007) respectively. This implies there was a source providing this mass at a rate of  $\sim 10^{-4}$  to  $10^{-2} M_\odot \text{ yr}^{-1}$ . We note that the Bondi accretion rate is comparable to the lower range of the rate needed to form the star cluster, suggesting that the SMBH itself may influence the rate of star formation in its immediate surroundings (see also Fatuzzo & Melia (2009) concerning this issue with regard to the Galactic center). Of course, suggesting that Bondi accretion is important begs the question of where the gas that is being accreted came from in the first place. We also note the co-incidence between the suggested age of the P3 star cluster (200 Myr) and the time of the last crossing of M32 through the nuclear region of M31 Block et al. (2006), suggesting that this crossing may have provided the trigger for the star formation event which formed the UV bright cluster at P3.

#### 4. Conclusions

We have detected X-ray emission from both optical nuclei of M31 (P1 and P3) and this variable emission is consistent with two point sources. Having resolved M31\* from the surrounding point and diffuse X-ray sources we can now investigate the accretion properties of this nearby SMBH. The presence of a hot and truly diffuse emission component in the core of M31 was first noted in *Einstein* observations (Trinchieri & Fabbiano 1991) and later confirmed with *ROSAT* (Primini et al. 1993), XMM-Newton (Shirey et al. 2001a), and *Chandra* (Dosaj et al. 2002) observations. Any of this gas within the Bondi radius of the SMBH will accrete and possibly generate accretion luminosity. In order to compute the Bondi accretion rate we use the X-ray observations to estimate the temperature and density of this gas. The resulting rate accretion rate would produce a luminosity of  $4 \times 10^{41} \text{ erg s}^{-1}$  if the gas radiated with the canonical  $\sim 10\%$  efficiency. Given the observed luminosity of  $\sim 2 \times 10^{36} \text{ erg s}^{-1}$ , M31\* is one of the most under-luminous SMBHs known.

Because M31\* has the most highly resolved Bondi flow of any SMBH, a long X-ray observation could determine the applicability of ADAF, CDAF, ADIOS, or other models to quiescent SMBH accretion. This in turn will tell us the form that black hole accretion takes for the vast majority of cosmic time. For example, a 400 ks ACIS-S observation would yield 2500 counts within the Bondi radius (nearly 10 per pixel), sufficient to divide the region into 5 annuli and determine accurate temperatures in 5 radial rings. This would be sufficient to determine the run of temperature with radius in the RIAF. The various RIAF models all predict  $T (1/r)^\alpha$ , so these data could determine  $\alpha$  and therefore the structure of the RIAF.

## 5. Acknowledgments

This work was supported in part by *Chandra* Grant GO-6088A and Chandra X-ray Center Contract NAS8-03060.

Chandra HST(ACS)

## REFERENCES

- Baganoff, F. K., Bautz, M. W., Brandt, W. N., Chartas, G., Feigelson, E. D., Garmire, G. P., Maeda, Y., Morris, M., Ricker, G. R., Townsley, L. K., & Walter, F. 2001, *Nature*, 413, 45
- Baganoff, F. K., Maeda, Y., Morris, M., Bautz, M. W., Brandt, W. N., Cui, W., Doty, J. P., Feigelson, E. D., Garmire, G. P., Pravdo, S. H., Ricker, G. R., & Townsley, L. K. 2003, *ApJ*, 591, 891
- Barmby, P., Ashby, M. L. N., Bianchi, L., Engelbracht, C. W., Gehrz, R. D., Gordon, K. D., Hinz, J. L., Huchra, J. P., Humphreys, R. M., Pahre, M. A., Pérez-González, P. G., Polomski, E. F., Rieke, G. H., Thilker, D. A., Willner, S. P., & Woodward, C. E. 2006, *ApJ*, 650, L45
- Barmby, P. & Huchra, J. P. 2001, *AJ*, 122, 2458
- Beckerman, E., Aldcroft, T., Gaetz, T. J., Jerius, D. H., Nguyen, D., & Tibbetts, M. 2004, in Presented at the Society of Photo-Optical Instrumentation Engineers (SPIE) Conference, Vol. 5165, Society of Photo-Optical Instrumentation Engineers (SPIE) Conference Series, ed. K. A. Flanagan & O. H. W. Siegmund, 445–456
- Bender, R., Kormendy, J., Bower, G., Green, R., Thomas, J., Danks, A. C., Gull, T., Hutchings, J. B., Joseph, C. L., Kaiser, M. E., Lauer, T. R., Nelson, C. H., Richstone, D., Weistrop, D., & Woodgate, B. 2005, *ApJ*, 631, 280
- Blandford, R. D. & Begelman, M. C. 1999, *MNRAS*, 303, L1
- Block, D. L., Bournaud, F., Combes, F., Groess, R., Barmby, P., Ashby, M. L. N., Fazio, G. G., Pahre, M. A., & Willner, S. P. 2006, *Nature*, 443, 832
- Bogdan, A. & Gilfanov, M. 2008, ArXiv e-prints, 803
- Brown, R. L. & Lo, K. Y. 1982, *ApJ*, 253, 108
- Chang, P., Murray-Clay, R., Chiang, E., & Quataert, E. 2007, *ApJ*, 668, 236

- Crane, P. C., Dickel, J. R., & Cowan, J. J. 1993, *ApJ*, 411, L107+
- Demarque, P. & Virani, S. 2007, *A&A*, 461, 651
- Di Stefano, R., Kong, A. K. H., Greiner, J., Primini, F. A., Garcia, M. R., Barmby, P., Massey, P., Hodge, P. W., Williams, B. F., Murray, S. S., Curry, S., & Russo, T. A. 2004, *ApJ*, 610, 247
- Dosaj, A., Garcia, M., Forman, W., Jones, C., Kong, A., di Stefano, R., Primini, F., & Murray, S. 2002, in *ASP Conf. Ser. 262: The High Energy Universe at Sharp Focus: Chandra Science*, 147–+
- Dosaj, A., Garcia, M. G., Forman, W. R., Jones, C., Kong, A., Primini, F. A., Di Stefano, R., & Murray, S. S. 2001, in *Bulletin of the American Astronomical Society*, Vol. 33, *Bulletin of the American Astronomical Society*, 1369–+
- Edmonds, P. D., Gilliland, R. L., Heinke, C. O., & Grindlay, J. E. 2003, *ApJ*, 596, 1177
- Falcke, H. & Markoff, S. 2000, *A&A*, 362, 113
- Fatuzzo, M. & Melia, F. 2009, *PASP*, 121, 585
- Garcia, M. R., Kong, A., Primini, F. A., Barmby, P., Di Stefano, R., McClintock, J. E., & Murray, S. S. 2001, in *Two Years of Science with Chandra, Abstracts from the Symposium held in Washington, DC, 5-7 September, 2001*.
- Garcia, M. R., Murray, S. S., Primini, F. A., Forman, W. R., McClintock, J. E., & Jones, C. 2000, *ApJ*, 537, L23
- Garcia, M. R., Williams, B. F., Yuan, F., Kong, A. K. H., Primini, F. A., Barmby, P., Kaaret, P., & Murray, S. S. 2005, *ApJ*, 632, 1042
- Ghez, A. M., Duchêne, G., Matthews, K., Hornstein, S. D., Tanner, A., Larkin, J., Morris, M., Becklin, E. E., Salim, S., Kremenek, T., Thompson, D., Soifer, B. T., Neugebauer, G., & McLean, I. 2003a, *ApJ*, 586, L127
- . 2003b, *ApJ*, 586, L127
- Gordon, K. D., Bailin, J., Engelbracht, C. W., Rieke, G. H., Misselt, K. A., Latter, W. B., Young, E. T., Ashby, M. L. N., Barmby, P., Gibson, B. K., Hines, D. C., Hinz, J., Krause, O., Levine, D. A., Marleau, F. R., Noriega-Crespo, A., Stolovy, S., Thilker, D. A., & Werner, M. W. 2006, *ApJ*, 638, L87
- Hawley, J. F. & Balbus, S. A. 2002, *ApJ*, 573, 738

- Henze, M., Pietsch, W., Sala, G., Della Valle, M., Hernanz, M., Greiner, J., Burwitz, V., Freyberg, M. J., Haberl, F., Hartmann, D. H., Milne, P., & Williams, G. G. 2009, *A&A*, 498, L13
- Hornstein, S. D., Matthews, K., Ghez, A. M., Lu, J. R., Morris, M., Becklin, E. E., Rafelski, M., & Baganoff, F. K. 2007, *ApJ*, 667, 900
- Igumenshchev, I. V., Abramowicz, M. A., & Narayan, R. 2000, *ApJ*, 537, L27
- Kaaret, P. 2002, *ApJ*, 578, 114
- Kong, A. K. H., DiStefano, R., Garcia, M. R., & Greiner, J. 2003, *ApJ*, 585, 298
- Kong, A. K. H., Garcia, M. R., Primini, F. A., & Murray, S. S. 2002a, *ApJ*, 580, L125
- Kong, A. K. H., Garcia, M. R., Primini, F. A., Murray, S. S., Di Stefano, R., & McClintock, J. E. 2002b, *ApJ*, 577, 738
- Kormendy, J. & Bender, R. 1999, *ApJ*, 522, 772
- Lauer, T. R., Faber, S. M., Groth, E. J., Shaya, E. J., Campbell, B., Code, A., Currie, D. G., Baum, W. A., Ewald, S. P., Hester, J. J., Holtzman, J. A., Kristian, J., Light, R. M., Ligyns, C. R., O’Neil, E. J., & Westphal, J. A. 1993, *AJ*, 106, 1436
- Li, Z. & Wang, Q. D. 2007a, *ApJ*, 668, L39
- . 2007b, *ApJ*, 668, L39
- Li, Z., Wang, Q. D., & Wakker, B. P. 2009, *MNRAS*, 397, 148
- Liu, S. & Melia, F. 2001, *ApJ*, 561, L77
- Macquart, J.-P. & Bower, G. C. 2006, *ApJ*, 641, 302
- Marrone, D. P., Baganoff, F. K., Morris, M. R., Moran, J. M., Ghez, A. M., Hornstein, S. D., Dowell, C. D., Muñoz, D. J., Bautz, M. W., Ricker, G. R., Brandt, W. N., Garmire, G. P., Lu, J. R., Matthews, K., Zhao, J.-H., Rao, R., & Bower, G. C. 2008, *ApJ*, 682, 373
- Martins, F., Gillessen, S., Eisenhauer, F., Genzel, R., Ott, T., & Trippe, S. 2008, *ApJ*, 672, L119
- Massey, P., Olsen, K. A. G., Hodge, P. W., Strong, S. B., Jacoby, G. H., Schlingman, W., & Smith, R. C. 2006, *AJ*, 131, 2478

- Melia, F. 1992a, *ApJ*, 387, L25
- . 1992b, *ApJ*, 398, L95
- Narayan, R., Igemshchev, I. V., & Abramowicz, M. A. 2000, *ApJ*, 539, 798
- Narayan, R. & McClintock, J. E. 2008, *New Astronomy Review*, 51, 733
- Narayan, R. & Yi, I. 1994, *ApJ*, 428, L13
- . 1995, *ApJ*, 444, 231
- Pietsch, W., Haberl, F., Sala, G., Stiele, H., Hornoch, K., Riffeser, A., Fliri, J., Bender, R., Bühler, S., Burwitz, V., Greiner, J., & Seitz, S. 2007, *A&A*, 465, 375
- Prestwich, A. H., Irwin, J. A., Kilgard, R. E., Krauss, M. I., Zezas, A., Primini, F., Kaaret, P., & Boroson, B. 2003, *ApJ*, 595, 719
- Primini, F. A., Forman, W., & Jones, C. 1993, *ApJ*, 410, 615
- Quataert, E. & Gruzinov, A. 2000, *ApJ*, 539, 809
- Shirey, R., Soria, R., Borozdin, K., Osborne, J. P., Tiengo, A., Guainazzi, M., Hayter, C., La Palombara, N., Mason, K., Molendi, S., Paerels, F., Pietsch, W., Priedhorsky, W., Read, A. M., Watson, M. G., & West, R. G. 2001a, *A&A*, 365, L195
- . 2001b, *A&A*, 365, L195
- Shvartsman, V. F. 1971, *Soviet Astronomy*, 15, 377
- Sjouwerman, L. O., Kong, A. K. H., Garcia, M. R., Dickel, J. R., Williams, B. F., Johnson, K. E., Primini, F. A., & Goss, W. M. 2005, in *X-Ray and Radio Connections* (eds. L.O. Sjouwerman and K.K Dyer) Published electronically by NRAO, <http://www.aoc.nrao.edu/events/xraydio> Held 3-6 February 2004 in Santa Fe, New Mexico, USA, (E4.16) 4 pages, ed. L. O. Sjouwerman & K. K. Dyer
- Takahashi, H., Okada, Y., Kokubun, M., & Makishima, K. 2004, *ApJ*, 615, 242
- Tremaine, S. 1995, *AJ*, 110, 628
- Trinchieri, G. & Fabbiano, G. 1991, *ApJ*, 382, 82
- Trudolyubov, S., Kotov, O., Priedhorsky, W., Cordova, F., & Mason, K. 2005, *ApJ*, 634, 314

Williams, B. F., Garcia, M. R., McClintock, J. E., Kong, A. K. H., Primini, F. A., & Murray, S. S. 2005, *ApJ*, 628, 382

Williams, B. F., Naik, S., Garcia, M. R., & Callanan, P. J. 2006, *ApJ*, 643, 356